

Rotating disk apparatus for polymer-induced turbulent drag reduction[†]

Cheng Hai Hong¹, Hyoung Jin Choi^{1,*} and Jae Ho Kim²

¹Department of Polymer Science and Engineering, Inha University, Incheon 402-751, Korea

²Energy Conversion Department, Korea Institute of Energy Research, Daejeon 305-343, Korea

(Manuscript Received April 16, 2008; Revised July 7, 2008; Accepted July 23, 2008)

Abstract

In order to investigate turbulent drag reduction (DR), a rotating disk apparatus (RDA) generating an “external flow” was designed and then polymer-induced DR efficiency of water-soluble polymers both poly (ethylene oxide) (PEO) and poly (acryl amide) (PAAM) were examined as a function of either polymer concentration or temperature. The need for a sensitive measuring system at high Reynolds numbers has stimulated the development of a high-precision computer-aided system, which is able to measure the difference between the torques for a Newtonian fluid and a dilute polymeric solution with drag reducers very accurately. Their mechanical degradation behavior in the RDA as a function of time in a turbulent flow was also analyzed using both a simple exponential decay function and a fractional exponential decay equation. The fractional exponential decay equation was found to fit the experimental data better than the simple first-order degradation exponential decay function in the case of PEO.

Keywords: Drag reduction; Rotating disk apparatus; PEO; PAAM

1. Introduction

It is well known that under certain conditions of turbulent flow, the drag of a dilute polymer solution is drastically reduced by even minute amounts of suitable additives. This phenomenon implies that polymer solutions undergoing flow in a pipe require a lower pressure gradient to maintain the same flow rate. A higher flow rate would be obtained for the same pressure gradient if such an additive was used. While a satisfactory explanation of DR still eludes fundamental and general interpretation on it [1] due to a coupled mechanism of both turbulence [2] and polymer dynamics, the DR is reported to be governed by various parameters such as polymer concentration, polymer molecular weight, temperature, Reynolds number (N_{Re}), and solvent quality. The solvent effect which is related to polymer hydrodynamic volume

was found to play an important role on this DR phenomenon, such that coiled polymer molecules show a different type of drag reduction capability than extended ones [3, 4]. DR efficiency in good solvents has been found to be higher than that in poor solvents [5].

Among various theories and explanations on DR mechanism, viscoelastic interpretations of polymer added turbulent flows draw more attentions. Ruckenstein [6] reported two effects of viscoelasticity as main reasons of DR phenomenon. Using a Maxwell model as the constitutive equation for a viscoelastic fluid, he showed that the instantaneous shear stress at the wall in the viscoelastic fluid is smaller than in a corresponding Newtonian fluid. In addition, the replacement of the elements of liquid following short paths along the wall takes place as a result of turbulent fluctuations. In order to be replaced by other elements, an element moving along the wall must first relax its elastic stresses to enable viscous deformations required for its replacement to occur. This introduces a delay in the replacement process as compared to a Newtonian fluid. As the instantaneous shear

[†] This paper was presented at the 9th Asian International Conference on Fluid Machinery (AICFM9), Jeju, Korea, October 16-19, 2007.

*Corresponding author. Tel.: +82 32 860 7468, Fax.: +82 32 865 5178

E-mail address: hjchoi@inha.ac.kr

© KSME & Springer 2008

stress at the wall decreases for increasing contact times with the wall, the average shear stress at the wall decreases.

The importance of an elastic property to describe the mechanism of drag reduction was also examined [7]. Adopting a simple model to study both the turbulence and dissolved polymer molecules, the molecular dissipation to friction factors by constructing a self-consistent method was studied. For polymer molecules, a variant of the dumbbell model was adopted and a polymer molecule was found to grow by a factor of 10 or more from its equilibrium conformation which can absorb huge amount energy from the turbulent dissipation so that cutting turbulent eddy generation at certain length scale.

In this paper, we will not discuss the theoretical aspect of the origin of turbulent drag reduction but will focus on some empirical correlation among the molecular parameters for both water-soluble PEO and PAAM using a rotating disk apparatus (RDA). Generally various areas of application for the drag reduction phenomenon can be found both in tube flow and in rotating disk flow. Tube flow is related to engineering applications directly, such as crude oil transportation pipeline flow [8], irrigation systems, and treatment of blood circulation diseases [9]. On the other hand, external flow is also important for shipping industries with respect to increased velocity and fuel savings.

The RDA system investigated in this study is used to describe the external flow that includes the flow over flat plates as well as the flow around submerged objects. One studies typical friction drag for an internal flow, whereas the other studies the total drag of friction and form drag for an external flow. The drag reduction is known to be related only to the friction drag. Therefore, in order to study the total drag reduction, the rotating disk system is adopted in this study [10]. Because of this difference of the friction drag and the total drag between the tube flow and the rotating disk flow, a maximum of 80% of the drag reduction can be obtained from the tube flow, while the rotating disk flow generally produces about 50% of the maximum drag reduction [11].

On the other hand, the most effective drag-reducing polymers have a flexible and linear chain structure with a very high molecular weight [12–14]. However, the use of these high molecular weight polymers is limited due to their susceptibility to flow-induced degradation. Among the drag-reducing polymers,

high molecular weight water-soluble PEO and PAAM were selected for this study, in which both PEO and PAAM has been widely used as a drag reducer in aqueous systems [15].

Our aim in this study is to investigate the effects of two water-soluble polymers of PEO and PAAM on drag reduction and to characterize its drag reducing efficiency by using an RDA as a function of either temperature or concentration, because the concentration of a polymer solution has a significant effect on the drag reduction. In addition, their mechanical degradation behavior in the RDA as a function of time in a turbulent flow was also analyzed using both a simple exponential decay function and a fractional exponential decay equation.

2. Experimental

Concentrated stock solutions of both PEO (Sigma, USA, Mw-8,000,000) and PAAM (Sigma, USA, Mw-18,000,000) were separately injected into a water solution in the RDA. Stock polymer solutions (0.5 wt% concentration) were initially prepared by dissolving an appropriate amount of either PEO or PAAM in deionized water and then diluted to the required polymer concentration by carefully injecting measured quantities of stock solution directly into the turbulent flow field. Mild agitation was applied to both polymer systems to reduce mechanical degradation induced by stirring.

Fig. 1 shows a schematic diagram of the RDA. The fluid container consists of an aluminum cylinder, whose dimensions are 170 mm diameter \times 25 mm

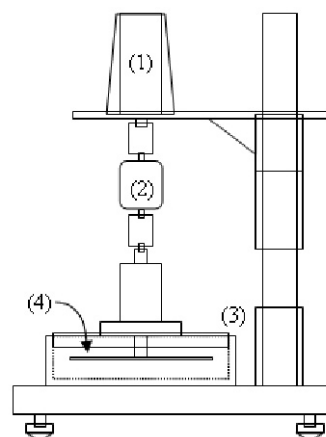


Fig. 1. (1) Motor (2) Torque sensor (3) Fluid container (4) Rotating disk.

wall thickness, and a removable 30 mm thick aluminum lid to seal the solution. A 20 mm diameter circle is bored in the center of the lid to allow the entry of a 15 mm diameter rotating shaft, which is supported by two bearings to avoid vibration at high N_{Re} . The disk, connected to a motor using the rotating shaft, has dimensions of 140 mm diameter \times 3 mm thickness and is located directly between the bottom of the cylinder and the lid. The volume of solution required to fill the container is approximately 0.4 liter. The temperature of the container is controlled using a circulating fluid bath jacket with a controlled temperature water bath.

The drive motor is supported by a cast iron frame, which ensures accurate positioning of the motor. The motor assembly (motor and loader) used to operate the disk consists of a 0.75 kW AC servo motor (model BM0730E3, Shinko Co., Japan), which is able to operate up to a maximum rotational speed of 3000 rpm with a very high rotational acceleration. The rotational speed and motor power control are determined by the loader (model: SSM-2075, Shinko Co., Japan). The loaded torque on the disk is detected using a model 01224-120 rotary shaft torque sensor (acquired from Sensor Developments Inc., Lake Orion, MI USA). It can measure the torque from 0 to 200 oz-in. (14.12×10^6 dyne-cm) with a 0.1% of full-scale non-linearity and 150% of full-scale overload capacity. One shaft of the torque sensor is coupled with the motor using a steel coupling, and the other is joined directly with the hollow disk shaft to monitor the torque. Two stainless-steel load-bearing assemblies support the shaft at both ends to reduce vibration, and the disk is connected to the other shaft. Therefore, the influence of the bearing assembly on detecting the torque must be verified by the torque difference between the pure solvent and polymeric solution.

The torque required to rotate the disk for pure solvent (T_s) at a given speed was measured first. The percent DR (%DR) was then calculated by measuring the corresponding torque required for a dilute polymer solution (T_p) at the same ω as:

$$\%DR = \left(\frac{T_s - T_p}{T_s} \right) \times 100 \quad (1)$$

Note that $N_{Re} = \rho r^2 \omega / \mu$ is based on the rotational speed of RDA, in which ρ is the fluid density, μ is the fluid viscosity, and r is the radius of the disk. The %DR was then obtained as a function of time.

The temperature of the system was maintained at 25 °C. Either PEO or PAAM was injected into the turbulent flow field for the DR measurement. The %DR was then obtained as a function of time by injecting measured quantities of stock solution directly into the turbulent flow field generated by the RDA.

The need for a sensitive measuring system at high Reynolds numbers has stimulated the development of a high-precision computer-aided system, which is able to measure the difference between the torques for a Newtonian fluid and a dilute suspension with drag reducers very accurately.

3. Results and discussion

Since drag reduction is caused by the sum of the contributions from individual polymer molecules, increasing concentrations of polymer solutions increase the amount of drag reduction. Fig. 2 shows the dependence of the %DR of PEO as a function of polymer concentration up to 10 wppm at RDA rotational velocity of 1980 rpm. The dependence of the percent drag reduction on PAAM as a function of polymer concentration up to 10 wppm at the rotational disk velocity of 1980 rpm was also determined as shown.

We also observed the stability of the polymer chain for different temperatures in a turbulent flow. Fig. 3 illustrates the temperature dependence of the %DR as a function of time. Even through the initial drag reduction is higher than those at any other temperature with PAAM. As the time progresses, higher drag reduction efficiency is observed at lower temperatures than that at higher temperatures. Meanwhile, higher DR efficiency is observed at mild temperature than

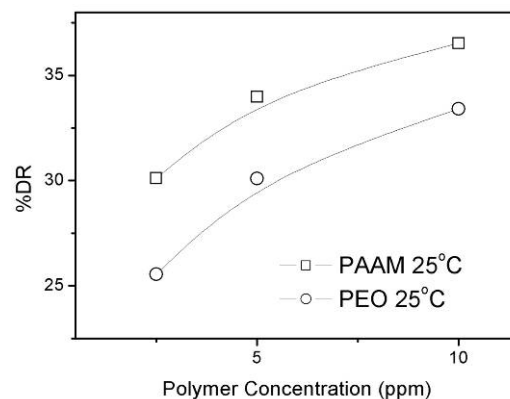


Fig. 2. Concentration effect of %DR for PEO and PAAM.

another temperatures with PEO.

Fig. 4 represents the time evolution of the DR efficiency at various concentrations with PEO and PAAM. For fixed PEO concentrations of 2.5, 5, and 10 ppm, the resulting DR efficiency were 25.54%, 30.09%, and 33.42%, respectively. In the same way, the resulting DR efficiency of PAAM were 30.12%, 33.98%, and 36.53%, respectively. The overall trend was a distinct decrease in the DR efficiency. Furthermore, the asymptote values were different for each concentration within a short time scale (<300 s), indicating their similar degradation mechanism.

On the basis of the results of the DR experiment at various concentrations, a numerical fitting was also conducted using the simple first-order degradation model. The degradation features at different concentration can be fitted and numerically expressed by the coefficients in Eq. (2) as a first-order approximation

where $w(L)$ is the drag reducing power dependence on L and c is the background contribution due to systematic uncertainties in the measurement.

$$\begin{aligned} \%DR(t) &= w(L)N_L(t) + w(L/2)N_{L/2}(t) + c \\ &= w_1e^{-\alpha t} + 2w_2(1-e^{-\alpha t}) + c \end{aligned} \quad (2)$$

Based on this equation, the physical interpretation of the DR and mechanical molecular degradation can be described using two time-independent parameters, α and w . The solid lines in Fig. 4 are obtained from nonlinear curve fitting for α and w using the simple first-order degradation model. The results are summarized in Table 1. As shown in Table 1, the rate constant (α) decreased with the concentration.

$$\frac{DR(t)}{DR_0} = \frac{1}{1 + W(1-e^{-ht})} \quad (3)$$

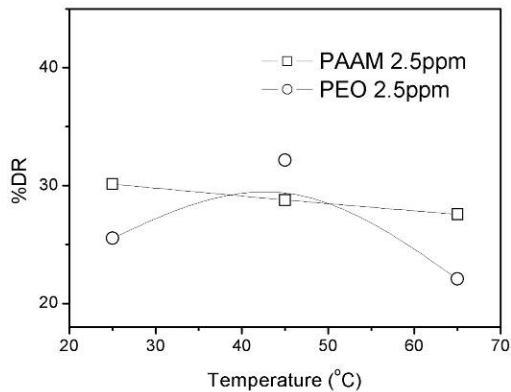


Fig. 3. Temperature effect of %DR for 2.5 ppm PEO and PAAM.

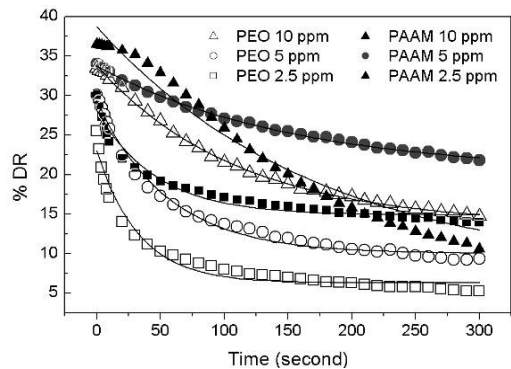


Fig. 4. %DR as a function of time for PEO and PAAM in solution at different concentrations, 25°C. Solid line represents values obtained from Eq. (2), and points represent experimental data.

Conversely, it should also be noted that in an effort to explain the relationship between drag reduction and molecular degradation, Brostow et al. [16] devel-

Table 1. results of initial stage data fitting for PEO and PAAM in solution at different concentration Using simple First-Order Degradation Model Eq. (2).

		w_1	w_2	α	c
PEO	2.5 ppm	22.42	2.83	0.0304	0.63
	5 ppm	27.57	4.09	0.0181	1.79
	10 ppm	32.28	6.02	0.0090	1.54
PAAM	2.5 ppm	23.12	4.94	0.0214	4.99
	5 ppm	25.68	6.08	0.0066	8.09
	10 ppm	32.29	0.49	0.0058	6.43

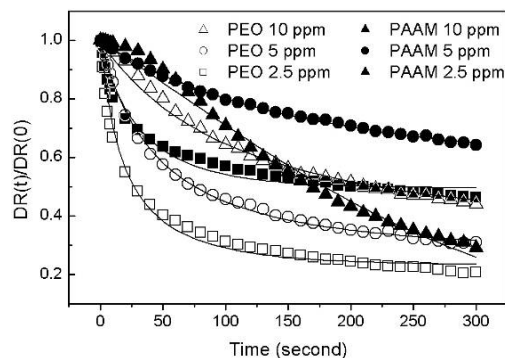


Fig. 5. $DR(t)/DR(0)$ as a function of time for PEO and PAAM in solution at different concentration, 25°C. Solid line represents values obtained from Eq. (3), and points represent experimental data.

Table 2. Results of initial stage data fitting for PEO and PAAM in solution at different concentration using fractional exponential decay equation (Eq. 3).

		W	h
PEO	2.5 ppm	2.4571	0.0069
	5 ppm	3.3185	0.0133
	10 ppm	1.8339	0.0035
PAAM	2.5 ppm	1.0196	0.0177
	5 ppm	0.8050	0.0037
	10 ppm	-0.4122	-0.0069

oped the following empirical exponential decay function with h as the decay constant. Considering the fact that the DR efficiency and mechanical degradation are related to the macromolecular conformation in the solution, the DR efficiency is known to be proportional to the molecular weight of the polymers. Thus, this DR efficiency ratio can be regarded as the ratio of the effective number-averaged molecular mass at time t and $t=0$ ($M(t)/M_0$). They also noted that the points on the chain scission. Depending on their specific location, some of these points may be protected from degradation by their surroundings, while others will undergo scission under a flow. In the latter case, the average number of points per chain is denoted by W , which is proportional to the number of breakable sequences with two different orientations, and also can be related to the drag reducer concentration [17]. A larger value of h indicates fast degradation, while a larger value of W implies a low shear stability. Such as PEO and PAAM with 2.5 ppm is possess larger values of h and W , i.e., possess fast degradation and low shear stability [18, 19]. And observed from Table 2. As a result, Fig. 5 shows that the degradation features at different concentration can be fitted and numerically expressed by the coefficients in Eq. (3) as a fractional exponential decay equation.

4. Conclusions

Using an RDA with a high-precision computer-aided system, the typical drag reduction experiments were performed using water-soluble polymers of PEO and PAAM as a function of polymer concentration and temperature. The experimental data were fitted by the simple first-order degradation exponential decay function and the fractional exponential decay equation.

Acknowledgments

This work was supported by the research grant from the KIER, Korea (2007).

References

- [1] Y. Amarouchene and H. Kellay, Polymers in 2D turbulence: Suppression of large scale fluctuations, *Phys. Rev. Lett.* 89 (10) (2002) 104502.
- [2] P. Tong, W. I. Goldburg, C. K. Chan and A. Sirivat, Turbulent transition by photon-correlation spectroscopy, *Phys. Rev. A* 37 (6) (1988) 2125-2133.
- [3] A. Nakano and Y. Minoura, Effects of solvent and concentration on scission of polymers with high-speed stirring, *J. Appl. Polym. Sci.* 19 (8) (1975) 2119-2130.
- [4] A. Nakano and Y. Minoura, Relationship between hydrodynamic volume and scission of polymer-chains by high-speed stirring in several solvents, *Macromolecules*, 8 (5) (1975) 677-680.
- [5] J. F. S. Yu; J. L. Zakin and G. K. Patterson, Mechanical degradation of high molecular-weight polymers in dilute-solution, *J. Appl. Polym. Sci.* 23 (8) (1979) 2493-2512.
- [6] E. Ruckenstein, Mechanism of drag reduction, *J. Appl. Polym. Sci.*, 17 (10) (1973) 3239-3240.
- [7] R. Armstrong and M. S. Jhon, A self-consistent theoretical approach to polymer induced turbulent drag reduction, *Chem. Eng. Commun.*, 30 (1984) 99-112.
- [8] E. D. Burger, L. G. Chorn and T. K. Perkins, Studies of drag reduction conducted over a broad range of pipeline conditions when flowing Prudhoe Bay crude-oil, *J. Rheol.*, 24 (5) (1980) 603-626.
- [9] H. L. Greene, R. F. Mostardi and R. F. Nokes, Effects of drag reducing polymers on initiation of atherosclerosis, *Polym. Eng. Sci.*, 20 (7) (1980) 499-504.
- [10] C. A. Kim, D. S. Jo, H. J. Choi, C. B. Kim and M. S. Jhon, A high-precision rotating disk apparatus for drag reduction characterization, *Polym. Test.*, 20 (1) (2001) 43-48.
- [11] P. Tong, W. I. Goldburg, J. S. Huang and T. A. Witten, Anisotropy in turbulent drag reduction, *Phys. Rev. Lett.*, 65 (22) (1990) 2780-2783.
- [12] H. J. Choi, S. T. Lim, P. Y. Lai and C. K. Chan, Turbulent drag reduction and degradation of DNA, *Phys. Rev. Lett.*, 89 (8) (2002) 088302.
- [13] S. T. Lim, H. J. Choi, S. Y. Lee, J. S. So and C. K.

- Chan, Gamma-DNA induced turbulent drag reduction and its characteristics, *Macromolecules*, 36 (14) (2003) 5348-5354.
- [14] S. T. Lim, S. J. Park, C. K. Chan and H. J. Choi, Turbulent drag reduction characteristics induced by calf-thymus DNA, *Physica, A* 350 (1) (2005) 84-88.
- [15] S. A. Vanapalli, M. T. Islam and M. J. Solomon, Scission-induced bounds on maximum polymer drag reduction in turbulent flow, *Phys. Fluids*, 17 (9) (2005) 095108.
- [16] W. Brostow; H. Ertepinar and R. P. Singh, Flow of Dilute Polymer-Solutions - Chain Conformations and Degradation of Drag Reducers, *Macromolecules*, 23 (24) (1990) 5109-5118.
- [17] S. T. Lim, C. H. Hong, H. J. Choi, P. Y. Lai and C. K. Chan, Polymer turbulent drag reduction near the theta point, *Euro. Phys. Lett.*, 80 (2007) 58003.
- [18] S. A. Vanapalli, S. L. Ceccio and M. J. Solomon, Universal scaling for polymer chain scission in turbulence, *PNAS*, 103 (45) (2006) 16660-16665.
- [19] H. J. Choi, C. A. Kim, J. I. Sohn and M. S. Jhon, An exponential decay function for polymer degradation in turbulent drag reduction, *Polym. Deg. Stab.*, 69 (2000) 341-346.